JOURNAL OF APPLIED PHYSICS **101**, 09K504 (2007)

^{119}Sn transferred hyperfine fields in $ErMn_6Sn_{6-x}Ga_x$

Laura K. Perry and D. H. Ryan[a)]
Centre for the Physics of Materials, McGill University, Montréal, Quebec H3A 2T8, Canada and Physics Department, McGill University, Montréal, Quebec H3A 2T8, Canada

G. Venturini
Laboratoire de Chimie du Solide Minéral, Université Henri Poincaré-Nancy I, Associé au CNRS (UMR 7555), BP 239, 54506 Vandoeuvre les Nancy Cedex, France

(Presented on 9 January 2007; received 16 October 2006; accepted 20 November 2006; published online 26 March 2007)

We present here the Sn anisotropic fields in $ErMn_6Sn_{5.89}Ga_{0.11}$, studied by ^{119}Sn Mössbauer spectroscopy. The moments undergo a 90° spin reorientation from the *ab* plane to the *c* axis on cooling through $T_{sr}=38(2)$ K. We find that the hyperfine field at Sn-2*c* is totally isotropic, while 5(1)% of B_{hf} at Sn-2*d* and more than 20% of B_{hf} at Sn-2*e* arise from anisotropic contributions. © *2007 American Institute of Physics*. [DOI: 10.1063/1.2709419]

I. INTRODUCTION

The hyperfine field (B_{hf}) observed at nonmagnetic probe sites in magnetically ordered materials must arise from the effects of surrounding magnetic moments. The transfer process is generally assumed to be isotropic, driven by the magnitude of the neighboring moments and their magnetic symmetry. However, where the bonding has a partially covalent character, the transferred hyperfine field includes an anisotropic contribution: B_{hf} also depends on the relative orientations of the moments and their connecting bonds. This anisotropic contribution can be a substantial fraction of the total transferred hyperfine field[1,2] and neglecting the anisotropic contribution to B_{hf} can lead to incorrect site assignments in multicomponent spectra. Attributing the component with the largest B_{hf} to the site with the most magnetic neighbors frequently fails to yield a correct interpretation of the observed spectrum.

To isolate the anisotropic contribution, we need to change the orientation of the surrounding magnetic moments without affecting their symmetry, positions, or magnitudes. In many of the ferrimagnetic RMn_6Sn_6 compounds, the moments undergo a spontaneous temperature-driven reorientation in which they rotate from the *ab* plane to the *c* axis on cooling through T_{sr}. The magnetic structures of these compounds are simple and provide three distinct Sn sites at which to study the anisotropic field. As the environment of each site is unique, the spin reorientation affects each Sn site differently. In $TbMn_6Sn_{6-x}Ga_x$,[3] the size ordering of hyperfine fields changes at T_{sr}, so that a site assignment based solely on the magnitudes of B_{hf} does not yield a unique result. Site assignments in this system must be based on the electrostatic environment (Δ), which is unaffected by the reorientation except for a uniform change by a factor of -2.

Although the moments in $ErMn_6Sn_6$ do not undergo a spin reorientation transition, the transition can be forced with a small amount of Ga doping ($x_{crit}=0.1$), and T_{sr} can be driven as low as 36 K (Ref. 4) (in $TbMn_6Sn_{6-x}Ga_x$, Ga doping decreases T_{sr} by ~ 255 K/Ga) where the thermal variation of the moments is negligible, resulting in a clean and simple spin reorientation. We present here a ^{119}Sn Mössbauer study of the transferred hyperfine fields in $ErMn_6Sn_{5.89}Ga_{0.11}$. We find that on cooling through $T_{sr}=38(2)$ K, the quadrupole splitting changes by a factor of -2, within error, for all three Sn sites, consistent with a full 90° rotation of the moments. From the change in B_{hf} through T_{sr}, we determine the anisotropic contributions to B_{hf} at each Sn site. Remarkably, more than 20% of the hyperfine field at one site (Sn-2*e*) arises from anisotropic contributions.

II. EXPERIMENTAL METHODS

The $ErMn_6Sn_{5.89}Ga_{0.11}$ single crystal was synthesized using a flux method similar to that previously reported in Ref. 5. Stoichiometric amounts of $ErMn_6Sn_6$ and elemental gallium (atomic ratio $ErMn_6Sn_{31.5}Ga_{0.5}$) were alloyed in an induction furnace. The resulting ingot was sealed under argon in a silica tube and annealed for two weeks at 1263 K. In $RMn_6Sn_{6-x}X_x$, smaller *R* and *x* yield larger single crystals. $ErMn_6Sn_{5.89}Ga_{0.11}$ grew as a large ($\sim 7\times 4\times 1$ mm^2), faceted, single crystal. Part of it was powdered for x-ray diffraction and Mössbauer spectroscopy. The compound is isotypic with the $HfFe_6Ge_6$-type crystal structure ($P6/mmm$ space group), with cell parameters $a=5.508(2)$ Å and $c=8.989(5)$ Å.[6] The crystal cleaves parallel to the *c* axis so that an oriented piece could be cut for magnetometry.

III. RESULTS AND DISCUSSION

The Mn sublattice of the ternary $ErMn_6Sn_6$ compound orders antiferromagnetically at $T_N=352$ K.[7] The material becomes ferrimagnetic when the Er sublattice orders at 75 K. With a small amount of Ga substitution, the $ErMn_6Sn_{5.89}Ga_{0.11}$ compound is ferrimagnetic over its whole ordered range below $T_N=372$ K. Figure 1 shows the magnetization ($T<60$ K) in an applied field of $B_0=1$ T, for B_0 both parallel (left) and perpendicular (right) to the *c* axis. The

---

[a)] Electronic mail: dominic@physics.mcgill.ca

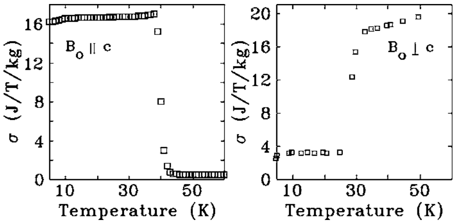

FIG. 1. Magnetization of $ErMn_6Sn_{5.89}Ga_{0.11}$ in an applied field of 1 T, parallel (left) and perpendicular (right) to the c axis.

anomaly at $T_{sr}=39(1)$ K marks the spin reorientation transition. The width of the transition is less than 1 K, so the reorientation is an abrupt, well-defined transition. T_{sr} is in close agreement with that measured in the polycrystalline $ErMn_6Sn_{5.8}Ga_{0.2}$ compound ($T_{sr}=36$ K).[4] The saturation magnetization [15.59(2) J/T kg] yields a Mn moment value of $\mu_{Mn}=2.1(1)\mu_B$, close to that derived from neutron scattering in $ErMn_6Sn_6$ [$\mu_{Mn}=2.21(5)\mu_B$] (Ref. 8) (the assumed Er moment is $\mu_{Er}=9\mu_B$).

In the $HfFe_6Ge_6$-type crystal structure, there are three Sn sites: Sn-2c (at the center of a trigonal rare earth plane), Sn-2d (with no rare earth neighbors), and Sn-2e (slightly offset from a hexagonal Mn_6 plane). Both Sn-2c and Sn-2d sit at the centers of Mn_6 hexagonal prisms. The 12 K Mössbauer pattern of $ErMn_6Sn_{5.89}Ga_{0.11}$ powder, shown in Fig. 2, was fitted with three subspectra (one for each Sn site) and a central Sn impurity [spectral area 2.4%, isomer shift $\delta=2.62(6)$ mm/s relative to $CaSnO_3$ at 295 K, and Debye temperature $\theta_D=165(5)$ K]. The areas of the three sextets were adjusted freely.

In order to observe the anisotropic effects at each of the three Sn sites, they must be correctly identified. For $T<T_{sr}$, B_{hf}(Sn-2d)$>B_{hf}$(Sn-2c). Therefore, the site with the three Er neighbors experiences a smaller transferred hyperfine field than the site with none. However, as we will later show in Fig. 3 (bottom right), the Sn-2c and Sn-2d fields exchange sequence on heating through T_{sr}, and thus the field ordering below T_{sr} differs from that above T_{sr}. Since we expect all moments in the structure to rotate by the same angle, the effect of the reorientation on the electrostatic environment is the same for each Sn site. Therefore, the site assignment is based on the sequence of quadrupole splittings, which is $|\Delta(\text{Sn-}2d)|>|\Delta(\text{Sn-}2c)|>|\Delta(\text{Sn-}2e)|$ for any temperature (Fig. 3, top right). The quadrupole splittings in $TbMn_6Sn_{6-x}Ga_x$ (Ref. 3) served as a guide for the site assignment (Table I).

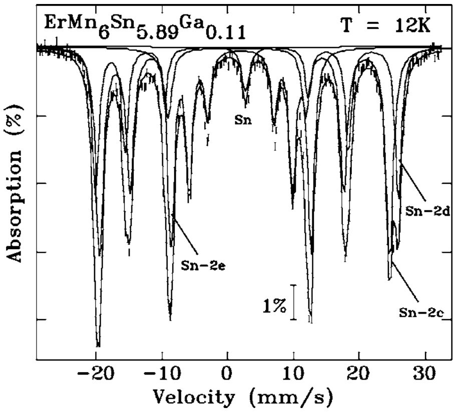

FIG. 2. Mössbauer spectrum for $ErMn_6Sn_{5.89}Ga_{0.11}$ at 12 K.

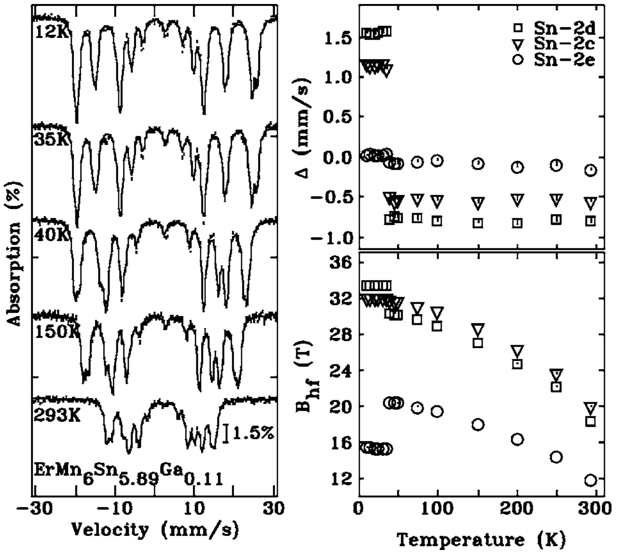

FIG. 3. Left: Mössbauer spectra of $ErMn_6Sn_{5.89}Ga_{0.11}$, from 12 to 300 K. Top right: Quadrupole splittings and bottom right: hyperfine fields at the three Sn sites in $ErMn_6Sn_{5.89}Ga_{0.11}$ ($12\text{ K}<T<300$ K). These yield a spin reorientation temperature of $T_{sr}=38(2)$ K.

Figure 3 (left) shows the evolution of the Mössbauer spectra with increasing temperature. The subspectral areas were constrained to those determined at 12 K. The change in the spectra between 35 and 40 K marks the spin reorientation transition, which is thus narrower than 5 K. Figure 3 (top right) shows the quadrupole splittings of the three Sn sites as functions of temperature, and $\Delta_{T<T_{sr}}=-2\Delta_{T>T_{sr}}$ within error for all three Sn sites (Table II). The moments thus rotate by 90° on cooling through $T_{sr}=38(2)$ K, from the ab plane to the c axis.

The temperature dependence of B_{hf} at the three Sn sites is shown in Fig. 3 (bottom right). On cooling through T_{sr}, B_{hf} decreases at Sn-2e and increases at Sn-2d, while there is very little change at Sn-2c. We can determine the anisotropic field directly from these changes in B_{hf}, since it alone is changed by the reorientation. The temperature dependence of B_{hf} for $T>T_{sr}$ ($\mu \perp c$) was fitted to a Brillouin curve and extrapolated to T_{sr}. The difference $B_{hf}^{\mu\parallel c}(T_{sr})-B_{hf}^{\mu\perp c}(T_{sr})$ was tracked back to 0 K in order to determine the change in hyperfine field due to the reorientation *at* 0 K, δB_{hf}. This change in B_{hf} is the anisotropic field, B_{hf}^A, given in the second column of Table III for each Sn site.

The first neighbors for all three Sn sites are Mn atoms,

TABLE I. Mössbauer parameters at 12 K in $ErMn_6Sn_{5.89}Ga_{0.11}$ and $TbMn_6Sn_{5.8}Ga_{0.2}$ (Ref. 3).

12 K Site	$ErMn_6Sn_{5.89}Ga_{0.11}$		$TbMn_6Sn_{5.8}Ga_{0.2}$	
	Δ (mm/s)	B_{hf} (T)	Δ (mm/s)	B_{hf} (T)
Sn-2c	1.17(2)	32.12(2)	1.11(1)	30.44(4)
Sn-2d	1.55(2)	33.56(2)	1.57(3)	32.94(4)
Sn-2e	0.03(2)	15.54(2)	0.16(1)	13.81(2)

TABLE II. Mössbauer parameters at 35 and 40 K in $ErMn_6Sn_{5.89}Ga_{0.11}$.

	$T<T_{sr}$ ($\mu \| c$) 35 K		$T>T_{sr}$ ($\mu \perp c$) 40 K	
Site	Δ (mm/s)	B_{hf} (T)	Δ (mm/s)	B_{hf} (T)
Sn-2*c*	1.11(2)	31.99(2)	−0.51(2)	31.87(2)
Sn-2*d*	1.54(3)	33.46(3)	−0.81(3)	30.33(2)
Sn-2*e*	0.07(2)	15.45(2)	−0.03(2)	20.53(2)

with the Er atoms further away.[9] The anisotropic contribution to B_{hf} is thought to arise through partially covalent bonding between the magnetic atoms and the Sn.[1,2] If we therefore ignore contributions to B_{hf} from second neighbor Er atoms (the observed fields here are comparable to those in alloys with nonmagnetic atoms in the Er position[10]), the transferred hyperfine field at the Sn sites is given by[1]

$$\mathbf{B}_{hf} = \left[A_p \sum_{i=1}^{6} \mathbf{u}_i(\boldsymbol{\mu}_i \cdot \mathbf{u}_i) - \frac{A_p}{3} \sum_{i=1}^{6} \boldsymbol{\mu}_i \right] + A_s \sum_{i=1}^{6} \boldsymbol{\mu}_i, \tag{1}$$

where $\mathbf{u}_i$ is the unit vector connecting each Sn atom to a specific Mn atom with moment $\boldsymbol{\mu}_i$, and A_p and A_s are the dipolar and contact fields due to a unit Mn moment. A_p is also referred to as the anisotropic constant. The last term in Eq. (1) is the isotropic contribution from the Mn shells around the Sn atoms, while the first two terms represent the anisotropic transferred hyperfine field. We will only consider the first term in Eq. (1), denoted as $\mathbf{A}_1$, as the second is independent of moment orientation. In the $HfFe_6Ge_6$-type crystal structure, the Mn–Sn bonds make angles of 35° (Sn-2*c* and Sn-2*d*) and 73° (Sn-2*e*) with the *c* axis, and in $ErMn_6Sn_{5.89}Ga_{0.11}$, the moments are in the *ab* plane for $T > T_{sr}$ and along *c* for $T < T_{sr}$. ΔA_1 is the change in $\mathbf{A}_1$ due to a rotation from the *ab* plane to the *c* axis and is listed in Table III (see Ref. 11 for a more detailed description of these constants). Since the signs of B_{hf}^A and $\Delta A_1/A_p$ agree for the three Sn sites, the anisotropic and isotropic contributions to B_{hf} must have the same sign. Finally, the anisotropic constant is calculated as $A_p = B_{hf}^A/\Delta A_1$ and values are given in Table III. From Eq. (1) we can determine the ratio A_p/A_s, and we find that the transferred hyperfine field at Sn-2*c* is totally isotropic, while B_{hf} at Sn-2*d* consists of a 5(1)% anisotropic contribution. By contrast, the anisotropic field constitutes more than 20% of the total transferred hyperfine field at Sn-2*e*.

TABLE III. Anisotropic field B_{hf}^A, change in $\mathbf{A}_1$ due to a rotation from the *ab* plane to the *c* axis (Ref. 11), and resulting anisotropic constants for the three Sn sites in $ErMn_6Sn_{5.89}Ga_{0.11}$. From magnetometry, $\mu = \mu_{Mn} = 2.1(1)\mu_B$.

Site	B_{hf}^A (T)	$\Delta A_1/A_p$	A_p (T/μ_B)
Sn-2*c*	0.20 (4)	2.96μ	0.03(1)
Sn-2*d*	3.1(1)	3.03μ	0.49(2)
Sn-2*e*	−5.1(1)	-2.31μ	1.04(1)

The anisotropic constants at the Sn sites in $ErMn_6Sn_{5.89}Ga_{0.11}$ are significantly smaller than A_p measured in $MnSn_2$ [$B_{hf}^A = 4.9(2)$ T yielding $A_p = 2.19(9)$ T/μ_B (Ref. 1)]. Additional anisotropic contributions from Er–Sn bonding [not accounted for in Eq. (1)] could possibly affect the apparent Mn–Sn anisotropic contribution in this system, leading to smaller derived anisotropic constants. An investigation into this possibility is currently underway in the $YMn_6Sn_{6-x}In_x$ system.

The significant effect of the anisotropic field on the total measured hyperfine field at each site emphasizes the importance of including this term when interpreting the observed spectra. For example, site assignments based simply on matching the sequence of fields with the number of magnetic neighbors (more neighboring moments imply bigger field) fail here as the Sn-2*d* and Sn-2*c* change order on cooling through $T_{sr} = 38(2)$ K. Furthermore, the Sn-2*c* site has the most magnetic neighbors (six Mn and three Er) but has a smaller field (below T_{sr}) than the Sn-2*d* site which has only six Mn neighbors.

IV. CONCLUSIONS

Magnetization and ^{119}Sn Mössbauer spectroscopy have been used to show that anisotropic contributions to the transferred hyperfine field in $ErMn_6Sn_{5.89}Ga_{0.11}$ can be as much as 20% of the total observed field.

[1] G. Le Caër, B. Malaman, G. Venturini, and I. B. Kim, Phys. Rev. B **26**, 5085 (1982).
[2] G. Venturini and B. Malaman, Phys. Rev. B **35**, 7038 (1987).
[3] L. K. Perry, D. H. Ryan, G. Venturini, and J. M. Cadogan, J. Appl. Phys. **99**, 08J302 (2006).
[4] J.-L. Yao, S.-Y. Zhang, J. Du, M. Yan, D.-R. Yang, L.-G. Zhang, S.-M. Liu, and B.-G. Shen, Phys. Rev. B **67**, 134423 (2005).
[5] D. Clatterbuck and K. A. Gschneidner, Jr., J. Magn. Magn. Mater. **207**, 79 (1999).
[6] The composition of the crystal was verified using an SX50 electron probe at the Service Commun des Ondes Électroniques de l'Université de Nancy I-Henri Poincaré.
[7] G. Venturini, B. Chafik El Idrissi, and B. Malaman, J. Magn. Magn. Mater. **94**, 35 (1991).
[8] B. Malaman, G. Venturini, R. Welter, J. P. Sanchez, P. Vulliet, and E. Ressouche, J. Magn. Magn. Mater. **202**, 521 (1999).
[9] B. Chafik El Idrissi, G. Venturini, and B. Malaman, Mater. Res. Bull. **26**, 432 (1991).
[10] T. Mazet, J. Tobola, G. Venturini, and B. Malaman, Phys. Rev. B **65**, 104406 (2002).
[11] L. K. Perry, D. H. Ryan, and G. Venturini, Hyperfine Interact. (in press).